Bull. Chem. Soc. Jpn., ***68***, *1345—1351(1995)*

Mechanism of Sulfur Inversion in Sulfide Complexes of Gold(I) and Gold(III)

Shinji Toyota* and Michinori Ōki

Department of Chemistry, Faculty of Science, Okayama University of Science, Ridaicho, Okayama 700

(Received January 20, 1995)

Kinetic parameters for the sulfur inversion in various gold chloride complexes of alkyl benzyl sulfides were measured by the dynamic NMR method in order to obtain conclusive evidence for the inversion mechanism. A feature of kinetic data is that entropies of activation are nearly zero both in the gold(III) and gold(I) complexes, this suggesting that the sulfur inversion takes place via pyramidal inversion mechanism without breakage of the Au–S coordination bonds but not the dissociative mechanism. The negligible solvent effect on the inversion rates in the gold(III) and gold(I) complexes supports this mechanism as well. The barrier to sulfur inversion is higher by 2.9 kcal mol^{-1} in the gold(III) complexes than in the corresponding gold(I) complexes. The formal gold(II) complex exists as 1 : 1 mixture of gold(I) and gold(III) complexes in solution, each of them showing the dynamic behavior independently. The effect of oxidation state of the central gold atom on the sulfur inversion is discussed on the basis of MO calculation.

Inversion at sulfur atoms in metal-sulfide complexes has been extensively studied by taking advantage of the dynamic NMR method.[1—4] Generally two mechanisms are possible for the sulfur inversion. One is simple inversion without bond breakage (pyramidal inversion) and the other is a mechanism via dissociation of metal–sulfur bond (dissociative mechanism). We have shown that entropy of activation is one of the convenient clues to distinguish the two mechanisms: Entropy of activation is nearly zero ($\Delta S^{\neq}\approx 0$) in the pyramidal inversion and large and positive ($\Delta S^{\neq}\gg 0$) in the dissociative mechanism (Scheme 1).[5—8] By applying the rule, mechanisms of sulfur inversion were established not only in metal–sulfur complexes[6—8] but also in other trivalent sulfur compounds such as sulfonium salts.[5]

Despite the large number of investigations on the stereodynamics of sulfur ligands in transition metal complexes, there is only one paper that mentions sulfur inversion in gold complexes to the best of our knowledge. Coletta et al. obtained kinetic parameters for sulfur inversion in trichloro(dibenzyl sulfide)gold(III) (**1**) by the dynamic NMR method, where the entropy of activation was 9.5 cal mol^{-1} K^{-1} (1 cal=4.184 J), a positive value rather than nearly zero.[9] Although they tentatively concluded that the inversion took place by the pyramidal inversion mechanism, they could not rule out the possibility of other mechanisms such as the dissociative mechanism and the inversion accompanied by reduction–oxidation of gold atoms from the available data.

Because experimental errors in entropies of activation are usually larger than those in other kinetic parameters, careful measurements are necessary to obtain reliable values for the kinetic parameters. From our experiences, entropies of activation obtained by the total line shape analysis are reliable enough for quantitative discussion if certain requirements are met in the measurements and analyses.[10—12] Hence, we decided to remeasure the kinetic data of the sulfur inversion in the gold complexes in order to confirm the reliability of entropy of activation, which will provide further evidence for the inversion mechanism.

Coletta et al. also reported the dynamic behavior about a sulfur atom in gold(I) chloride–dibenzyl sulfide complex (**2**).[9] Although broadening of the ^{1}H NMR signal due to the benzylic methylene protons was observed at low temperatures, they failed to determine kinetic data because of a very small difference in the chemical shifts of the two diastereotopic protons. We felt that the use of a high-field NMR spectrometer or variation in solvents should allow us to measure the kinetic data of sulfur inversion in the gold(I) complex. Little is known about the effect of the oxidation state of the metal on the barrier to sulfur inversion except an example of platinum complexes.[1] Accordingly, a comparison of the kinetic data for the gold(III) and gold(I) complexes will be interesting and will lead us to get into insight of the effect of the charges on the metal atom.

In this paper, the kinetic parameters of the sulfur inversion in gold-sulfide complexes at two oxidation states are presented. The mechanism of the inversion is discussed on the basis of the features of the entropies of activation and solvent effect. The effect of the oxidation state of the gold atoms is also discussed with the aid of molecular orbital calculations of model complexes.

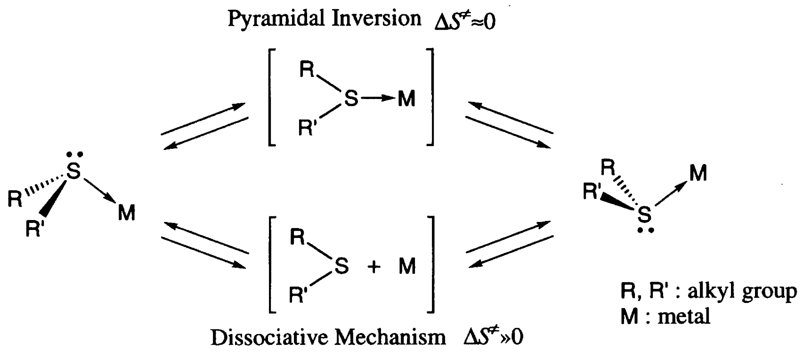

Scheme 1.

Results and Discussion

Synthesis. Gold complexes with dibenzyl sulfide ligand **1**—**3** were synthesized according to the procedure reported in the literatures.[13,14] Benzyl ethyl sulfide complexes were synthesized by a modified method. Treatment of gold(III) chloride with three equivalents of the sulfide in ethanol afforded white gold(I) complex **5**. This complex was oxidized by aqua regia to give the corresponding gold(III) complex **4** which was obtained as yellow crystals.

$[AuCl_3\{S(CH_2C_6H_5)_2\}]$ (**1**)
$[AuCl\{S(CH_2C_6H_5)_2\}]$ (**2**)
$[Au_2Cl_4\{S(CH_2C_6H_5)_2\}_2]$ (**3**)
$[AuCl_3\{S(CH_2C_6H_5)Et\}]$ (**4**)
$[AuCl\{S(CH_2C_6H_5)Et\}]$ (**5**)

Sulfur Inversion in Gold(III) Complexes. ^1H NMR signal due to the benzylic methylene protons in **1** appeared as a sharp AB quartet at room temperature, this suggesting that the sulfur inversion was frozen on the NMR time scale. The signal began to broaden as the temperature was increased and coalesced at ca. 80 °C, where the complex decomposed to some extent. The total line shape analysis of these line shape changes by the DNMR3K program[15] gave the kinetic parameters for the site exchange of the benzylic methylene protons, namely the sulfur inversion. Since the chemical shift difference of the methylene protons drifted with the temperature change, the values at temperatures where line shape changed was corrected for the computer simulation in a usual manner (see Experimental). Our previous works reveal that the analysis with the correction provides more reliable kinetic data, specially in the case where the drifting of the chemical shift is large.[5—8,12]

Kinetic parameters obtained for a chloroform-*d* solution are listed in Table 1. The free energy of activation for the sulfur inversion in **1** is 16.9 $\mathrm{kcal\,mol^{-1}}$ at 300 K, in good agreement with the reported value,[9] whereas the entropy of activation we have obtained (-0.5 $\mathrm{cal\,mol^{-1}\,K^{-1}}$) is nearly zero and significantly smaller than the literature value.[9] This discrepancy in the $\Delta S^{\neq}$ values is mainly attributed to the correction of the chemical shift differences.

In order to see whether the small entropy of activation is general or not for this type of compounds, we measured the kinetic parameters in another Au(III) complex. Benzyl ethyl sulfide complex **4** was chosen for the measurement for the following reasons. Firstly, this complex has a comparable stability to the dibenzyl sulfide complex and is expected to survive in a solution at high temperatures during the measurements. Secondly, the complex accommodates two probes for the line shape analysis, the benzylic methylene and ethylmethylene protons, in which the diastereotopic protons mutually exchange the sites on the sulfur inversion. The analysis with multiple probes is useful for estimating the reliability of kinetic data. Moreover, the methylene protons in the ethyl group has a relatively complicated exchange system, $ABX_3 \rightleftarrows BAX_3$. The line shape analysis with complicated signals tends to give more reliable kinetic data than that with simple ones.[12]

As shown in Table 1, the kinetic data obtained from the two probes in **4** are in good agreement with each other. The free energy of activation is slightly larger than that in the dibenzyl sulfide complex (**1**), this meaning that the effect of substitution of an ethyl group for a benzyl group is rather small. The entropies of activation are again nearly zero as was in complex **1**. These data enable us to confirm the reliability of values of entropy of activation; nearly zero entropy of activation is common to the sulfur inversion in the gold(III)–sulfide complexes.

It is possible to argue that the sulfur inversion in the gold(III) complexes is accomplished via the reductive elimination to $[AuCl\{S(CH_2C_6H_5)_2\}]$ and Cl_2, facile inversion about sulfur atom coordinating to the gold(I) atom as mentioned in the next section, and oxidative addition of chlorine. In this case, the plausible rate-limiting step is the first step. If this mechanism were important in the inversion process, the entropy of activation would have been a large value because of collapse of one molecule into two at the transition state. The observed values for the entropies of activation make it possible to rule out the process involving the reversible reduction–oxidation.

Solvent effect is another clue to elucidate the mecha-

Table 1. Kinetic Parameters for Sulfur Inversion in Gold–Sulfide Complexes **1**—**5** Measured in $CDCl_3$a)

Compound	$\Delta H^{\neq}$/kcal mol^{-1}	$\Delta S^{\neq}$/cal mol^{-1} K^{-1}	$\Delta G^{\neq}_{300}$/kcal mol^{-1}	rb)
1	16.7±0.4	−0.5±1.1	16.9	0.9998
2	14.7±0.3	2.1±0.8	14.0	0.9998
3c)	17.8±0.5	3.0±1.4	16.9	0.9996
3d)	15.4±0.5	4.4±1.5	14.0	0.9997
4e)	18.1±0.6	2.7±1.7	17.3	0.9996
4f)	17.8±0.4	1.8±1.3	17.3	0.9998
5e)	13.6±0.3	−2.0±1.1	14.2	0.9997
5f)	13.9±0.3	−0.8±1.0	14.1	0.9998

a) 1 cal=4.184 J. Concentration ca. 50 mmol L^{-1}. b) Correlation coefficient for the Eyring plot. c) Values for sulfur ligands coordinating to Au(III). d) Values for sulfur ligands coordinating to Au(I). e) Obtained from the benzylic methylene protons. f) Obtained from the ethyl-methylene protons.

nism of the sulfur inversion.7,8) The effect of solvents on the inversion rate is usually insignificant when the inversion proceeds without dissociation, while a significant solvent effect, such that polar solvents enhance the barrier height, is observed for the dissociative mechanism even though the extent of the solvent effect is small. In order to examine the solvent effect on rates of sulfur inversion in the gold complex, we determined the kinetic parameters for **1** in various solvents.

Because the gold(III) complex, which is a strong oxidizing reagent, apts to oxidize solvent, selection of solvents was limited. For example, when the gold(III) complex (**1**) was dissolved in ethanol or acetone, it tended to decompose to the corresponding gold(I) complex after a short time. We managed to obtain kinetic parameters, other than a chloroform-*d* solution, in aromatic hydrocarbons, benzene-d_6 and toluene-d_8 as shown in Table 2. So far as the data for the three solvents, there is no solvent effect on the kinetic data for sulfur inversion, this being in accord with the pyramidal inversion mechanism.

Sulfur Inversion in Gold(I) Complexes. Gold(I) chloride–dibenzyl sulfide complex (**2**) gave a singlet for ^{1}H NMR signal due to the benzylic methylene protons in chloroform-*d* at room temperature, whereas the signal became an AB quartet at −40 °C. The chemical shift difference, 13 Hz at 400 MHz, was so small that Coletta et al. had naturally failed to observe the signal splitting with a 90 MHz spectrometer.9) This line shape change is also attributable to the dynamic process of the inversion at the sulfur ligand. The kinetic parameters were similarly obtained by the line shape analysis.

Table 1 shows that the barrier height to sulfur inversion in **2** is lower by 2.9 kcal mol^{-1} than that in **1**: In other words, the sulfur inversion takes place 120 times faster in the gold(I) complex than in the gold(III) complex at 300 K. There has been little information on the effect of oxidation state of the central metals on the sulfur inversion energies. For platinum complexes, platinum(IV) complexes usually give higher barriers to inversion by 1—2 kcal mol^{-1} than platinum(II) complexes.1,17) The tendency, that the higher oxidation states of the central metal, the higher the barrier to sulfur inversion, is held in the gold complexes as well as in the platinum complexes. This point is discussed later with assistance of MO calculations.

Kinetic data for the gold(I)–benzyl ethyl sulfide complex (**5**) were determined for the same reasons mentioned in the previous section. The two probes gave essentially the same kinetic data as was in complex **4**. The free energy of activation is smaller by ca. 3 kcal mol^{-1} than that in the corresponding gold(III) complex (**4**). This energy difference is comparable to the case of dibenzyl sulfide complexes. Comparing the kinetic data of the complexes **2** and **5** in chloroform, one can notice that the effect of substituents on the sulfur atom is negligible in the gold(I) complexes.

The entropies of activation are nearly zero for all cases in the gold(I) complexes, this leading us to conclude that the configuration of the sulfur atom inverts without bond dissociation. We attempted to obtain the data for complex **2** in various solvents, but satisfactory data could be obtained only in halogenated hydrocarbons for several problems such as low solubility and decomposition of the complex. The chemical shift difference of the diastereotopic protons was so small in acetone-d_6 that the rate of inversion was determined by the coalescence method only at one temperature. There seems to be no solvent effect on the rates of the sulfur inversion in the gold(I) complex for the three solvents.

Sulfur Inversion in Formal Gold(II) Complex. It is known that the gold(II) complex (**3**) consists of an equimolar mixture of gold(I) and gold(III) complexes and that the mixed-valence gold atoms are arranged alternatively through one dimensional columns according to the crystallographic and theoretical studies.18—20)

^{1}H NMR spectrum of **3** gave two sets of signals due to the benzylic methylene protons at δ=4.14 and 4.46 in 1 : 1 ratio corresponding to the gold(I) and gold(III) complexes, respectively. These line shapes also depended on the measured temperature and the total line shape analysis gave the exchange rates individually

Table 2. Solvent Effect on Kinetic Parameters for Sulfur Inversion in Trichloro(dibenzyl sulfide)-gold(III) (**1**) and Chloro(dibenzyl sulfide)gold(I) (**2**)[a)]

Compound	Solvent	$\Delta H^{\neq}$/kcal mol^{-1}	$\Delta S^{\neq}$/cal mol^{-1} K^{-1}	$\Delta G^{\neq}_{300}$/kcal mol^{-1}	r[b)]
1	$CDCl_3$	16.7±0.4	−0.5±1.1	16.9	0.9998
1	C_6D_6	16.7±0.3	−0.5±0.9	16.9	0.9998
1	Toluene-d_8	16.7±0.4	−0.5±1.0	16.9	0.9997
2	$CDCl_3$	14.7±0.3	2.1±0.8	14.0	0.9998
2	CD_2Cl_2	14.9±0.4	3.3±1.3	13.9	0.9998
2	Acetone-d_6			14.0[c)]	

a) Concentration ca. 50 mmol L^{-1}. b) Correlation coefficient. c) Value at the coalescence temperature (−14.5 °C).

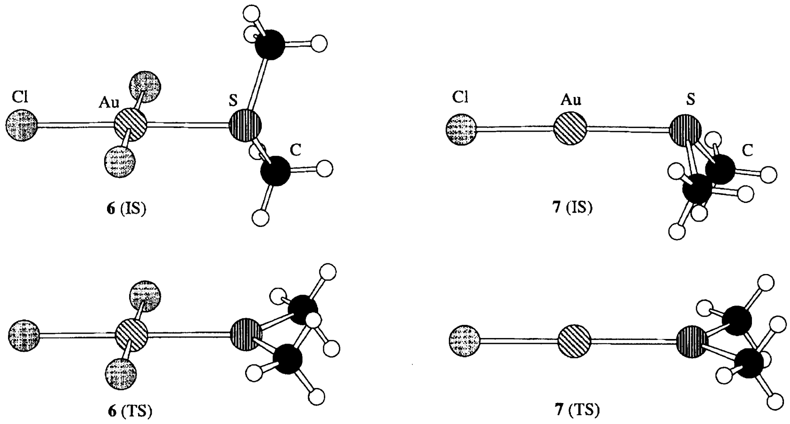

Scheme 2. Calculated structures at the initial state (IS) and the transition state (TS) for the sulfur inversion in trichloro(dimethyl sulfide)gold(III) (**6**) and chloro(dimethyl sulfide)gold(I) (**7**).

(Table 1). The kinetic parameters obtained from the signal at the lower and higher fields are in good agreement with those for complexes **1** and **2**, respectively. This means that the formal gold(II) complex retained the structure of the gold(I) and gold(III) complexes in a solution, where the sulfur inversion takes place independently in the two species. The inversion rates are scarcely affected by the presence of a gold complex of another oxidation state.

We wish to conclude from these experimental data that the sulfur inversion proceeds via pyramidal inversion mechanism in the gold–sulfide complexes whichever oxidation state the gold atom takes. This mechanism is also reasonable on the grounds of strong coordination bonds between the gold and sulfur atoms, where the back donation enhances the bond strength. The dissociation of the coordination bonds should require much more energy than the activation energies obtained here. Application of the relationship between the entropy of activation and the mechanism of sulfur inversion in the gold complexes has been proved useful.

MO Calculation. In order to get further insights into the differences in the sulfur inversion energy in the gold(I) and gold(III) complexes, ab initio molecular orbital calculations[21)] were performed for model compounds, $[AuCl_3(SMe_2)]$ (**6**) and $[AuCl(SMe_2)]$ (**7**). Calculations were carried out for the initial and transition states of the sulfur inversion with the LANL1DZ basis set, which accommodated parameters for a gold atom.[22—24)] The optimized structures are shown in Scheme 2 and total energies and selected structural parameters in Table 3.

Table 3. Total Energies and Structural Parameters of Optimized Structure for the Initial State (IS) and Transition State (TS) of Sulfur Inversion in Complexes **6** and **7**[a)]

	Energy/Hartree	Bond distance/Å		Bond angle/° [b)]
		Au–S	S–C	
6 (IS)	−166.60739	2.555	1.871	310.8
6 (TS)	−166.59276	2.593	1.867	360 (fixed)
ΔE[c)]	0.01462 (9.2)			
7 (IS)	−137.24561	2.558	1.868	314.0
7 (TS)	−137.23432	2.604	1.862	360 (fixed)
ΔE[c)]	0.01129 (7.1)			

a) Calculated by Gaussian92 program with the use of the LAND1DZ basis set. b) Sum of three bond angles around the sulfur atom. c) Energy difference between the initial state and transition state. Values in parentheses are energies in kcal mol^{-1}.

For the initial (ground) state, full optimization gave a square planar geometry for **6** and a linear for **7** around the gold atoms. The configurations around the sulfur atoms are pyramidal both in the gold(III) and gold(I) complexes at the initial state. The extent of the pyramidality is essentially the same in the two complexes as judged from the sum of the three bond angles around the sulfur atom. The calculated Au–S bond lengths are longer by 0.2—0.3 Å than the experimental values of the dibenzyl sulfide complexes determined by the X-ray analysis (ca. 2.30 Å).[25,26] This large discrepancy, which often happens in the calculation of molecules containing heavy atoms, may be due to deficiencies of the basis set.[27] We assume that the values are useful if we confine ourselves to discuss differences but not absolute values.

For calculation of transition states, the configurations about the sulfur atoms were fixed at a planar geometry during the optimization. The structures of the AuCl and $AuCl_3$ moieties are virtually unchanged from the initial structures, though the Au–S bonds are slightly longer in the transition states than in the initial state. In the gold(III) complex, the rotation about the Au–S bond takes place by ca. 90° from the initial state, this conformation being consistent with the X-ray structure of the dibenzyl sulfide complex (**1**).[25] We consider that this conformational change is not an important process in determining the inversion barrier because the bond rotation usually requires much lower energy than the sulfur inversion.

The energy differences between the initial and transition states are calculated as 9.2 and 7.1 $\mathrm{kcal\,mol^{-1}}$ for the gold(III) and gold(I) complexes, respectively. The calculation reproduces the effect of the oxidation state on the inversion energy, the barrier in the gold(III) complex being higher by 2.1 $\mathrm{kcal\,mol^{-1}}$ than that in the gold(I) complex. The calculated barrier heights are much smaller than the experimental values obtained for the dibenzyl sulfide complexes. These discrepancies are partly attributed to the lack of phenyl groups in the model compounds as well as to neglecting other factors such as solvation, but mainly to the immaturity of the basis set.

Previous calculations have shown that primitive basis sets do not satisfactorily reproduce inversion barriers of pyramidal nitrogen.[27] It is now shown that the theoretical prediction of barrier to sulfur inversion is also difficult with the LANL1DZ basis set, which contains several approximations for calculation of heavy metals. We may have to wait for correct prediction of barriers to inversion as well as exact geometry of the gold complexes until better methods of calculation become available.

Experimental

Gold–dibenzyl sulfide complexes **1**—**3** were prepared by the known method reported previously.[13,14] ^{1}H NMR data are as follows. Trichloro(dibenzyl sulfide)gold(III) (**1**): ^{1}H NMR ($CDCl_3$, r.t.) $\delta=4.29$ and 4.63 (4H, ABq, $J=13.0$ Hz), 7.04—7.48 (10H, m). Chloro(dibenzyl sulfide)gold(I) (**2**): ^{1}H NMR ($CDCl_3$, r.t.) $\delta=4.14$ (4H, br s), 7.38—7.43 (10H, m). Tetrachlorobis(dibenzyl sulfide)digold(II) (**3**): ^{1}H NMR ($CDCl_3$, r.t.) $\delta=4.14$ (4H, br s), 4.29 and 4.62 (4H, ABq, $J=13.0$ Hz), 7.37—7.44 (20H, app. s).

(Benzyl Ethyl Sulfide)chlorogold(I) (5). To a solution of benzyl ethyl sulfide (1.37 g or 9.00 mmol) in 40 mL of ethanol was added dropwise a solution of 1.00 g (3.00 mmol) of gold(III) chloride dihydrate in 20 mL of distilled water over 5 min at 0 °C. The mixture was stirred for 1 h at room temperature. The white precipitate was collected with a glass filter and washed with cold ethanol and then with diethyl ether. The solid was dried in vacuo and recrystallized from hexane–dichloromethane to give 0.88 g (75%) of white crystals. Mp 84.5—85.5 °C. Found: C, 28.02; H, 3.04%. Calcd for $C_9H_{12}AuClS$: C, 28.10; H, 3.14%. ^{1}H NMR ($CDCl_3$, r.t.) $\delta=1.42$ (3H, t, $J=7.4$ Hz), 2.91 (2H, q, $J=7.4$ Hz), 4.23 (2H, s), 7.35—7.45 (5H, m).

(Benzyl Ethyl Sulfide)trichlorogold(III) (4). A suspension of 305 mg (0.794 mol) of (benzyl ethyl sulfide)-chlorogold(I) in 5 mL of aqua regia was stirred for 1.5 h at room temperature. The colorless solid gradually turned to yellow during the stirring. The mixture was poured into 50 mL of distilled water. The solid was collected by filtration and washed with cold distilled water. Recrystallization of the solid from benzene–hexane afforded 232 mg (64%) of the desired compound as yellow crystals. Mp 83.0—85.0 °C. Found: C, 25.40; H, 2.68%. Calcd for $C_9H_{12}AuCl_3S$: C, 25.52; H, 2.86%. ^{1}H NMR ($CDCl_3$, r.t.) $\delta=1.52$ (3H, t, X of ABX_3, $J=7.3$ Hz), 2.99 and 3.31 (2H, AB of ABX_3, $J_{AB}=13.1$ Hz and $J_{AX}=J_{BX}=7.3$ Hz), 4.41 and 4.61 (2H, ABq, $J=13.2$ Hz), 7.39—7.49 (5H, m).

Dynamic NMR Measurement. ^{1}H NMR spectra at various temperatures were measured on a JEOL GSX-400 spectrometer operating at 399.8 MHz. Temperatures were calibrated with chemical shift differences of methanol and 1,2-ethanediol samples. About 10 mg of a complex was dissolved in an appropriate solvent to make up a sample with concentration of ca. 50 $\mathrm{mmol\,L^{-1}}$. The total line shape analysis was performed by DNMR3K program[15] with an NEC-98 series computer. Because the gold complexes decomposed at high temperatures, the analyses were performed for the signals where the decomposition was insignificant. The line shapes were analyzed as an AB $\rightleftarrows$ BA system for the benzylic methylene protons and as an $ABX_3 \rightleftarrows BAX_3$ system for the methylene protons in the ethyl groups. Chemical shift differences and coupling constants were measured at

Table 4. Temperature Dependence of the Chemical Shift Difference, Coupling Constant, and T_2 of the Benzylic Methylene Protons

Compound	Solvent	$\Delta\nu_{AB}$/Hz [a]	J_{AB}/Hz [b]	T_2/s [c]
1	$CDCl_3$	$0.237t+132.8$	−12.9	0.23
1	C_6D_6	$0.839t+64.9$	−13.1	0.14
1	Toluene-d_8	$0.883t+58.5$	−13.0	0.21
2	$CDCl_3$	$0.057t+19.1$	−12.7	0.20
2	CD_2Cl_2	13.4[d]	−12.5	0.21
2[e]	Acetone-d_6	7.2	−12.2	0.20
3[f]	$CDCl_3$	$0.272t+129.7$	−12.8	0.22
3[g]	$CDCl_3$	19.2[d]	−13.1	0.17
4	$CDCl_3$	$0.204t+75.6$	−13.2	0.20
5	$CDCl_3$	$-0.121t+24.5$	−12.9	0.25

a) Difference in the chemical shifts due to the methylene protons (AB signal): $\Delta\nu_{AB}/\mathrm{Hz}=xt/^\circ\mathrm{C}+y$. b) Coupling constant between AB protons. c) Spin–spin relaxation times. d) The chemical shift difference is independent of temperature. e) Values at −14.5 °C. f) Values for sulfur ligands coordinating to Au(III). g) Values for sulfur ligands coordinating to Au(I).

Table 5. Rate Constants of Sulfur Inversion in Complexes **1**—**5**

Compound	Solvent	k/s^{-1} (temperature/°C)
1	$CDCl_3$	7.8 (36.1), 10.8 (40.1), 15.8 (44.1), 22.0 (48.1), 30.5 (52.1), 42 (56.1), 58 (60.1), 82 (64.1)
1	C_6D_6	7.6 (35.1), 12.2 (40.1), 18.0 (45.2), 28.5 (50.1), 43.0 (55.3), 66 (60.3), 94 (65.3), 140 (70.3), 195 (75.3)
1	Toluene-d_8	6.6 (34.5), 9.8 (39.4), 16.5 (44.5), 24.5 (49.4), 38.0 (54.3), 58 (59.8), 90 (65.3), 130 (70.5), 185 (75.5), 270 (81.1)
2	$CDCl_3$	3.5 (−19.7), 5.6 (−15.7), 9.0 (−11.7), 13.8 (−7.7), 21.5 (−3.8), 32.5 (0.2), 48 (4.1), 68 (8.1), 100 (12.0)
2	CD_2Cl_2	4.8 (−17.5), 7.6 (−13.4), 11.8 (−9.6), 18.5 (−5.5), 29 (−1.5), 44 (2.4), 62 (6.3)
2	Acetone-d_6	8.2 (−14.5)
3[a)]	$CDCl_3$	10.2 (39.5), 14.4 (43.3), 21.0 (47.2), 28.0 (50.9), 39 (54.7), 56 (58.6), 80 (62.5), 105 (66.3)
3[b)]	$CDCl_3$	5.5 (−14.1), 9.2 (−9.8), 15.5 (−5.4), 25.0 (−1.1), 40 (3.2), 60 (7.5), 90 (11.8)
4[c)]	$CDCl_3$	6.6 (41.4), 9.6 (45.4), 14.5 (49.4), 20.0 (53.4), 28.5 (57.6), 42 (61.7), 56 (65.6)
4[d)]	$CDCl_3$	6.7 (41.4), 9.8 (45.4), 14.5 (49.4), 20.0 (53.4), 29.0 (57.6), 40 (61.7), 56 (65.6)
5[c)]	$CDCl_3$	4.0 (−19.7), 6.2 (−15.7), 9.2 (−11.7), 13.6 (−7.7), 19.8 (−3.8), 29.0 (0.2), 46.5 (5.1), 74 (10.0), 120 (15.1)
5[d)]	$CDCl_3$	6.0 (−15.7), 9.0 (−11.7), 13.6 (−7.7), 20.0 (−3.8), 29.5 (0.2), 47.5 (5.1), 78 (10.0), 120 (15.1)

a) Values for sulfur ligands coordinating to Au(III). b) Values for sulfur ligands coordinating to Au(I). c) Obtained from the benzylic methylene protons. d) Obtained from the ethyl-methylene protons.

several temperatures where the exchange rate was approximately zero. The coupling constants were independent of the temperature. The chemical shift differences were linearly correlated with temperature and the corrected values by extrapolation were used. Spin–spin relaxation times were estimated from the line shapes at the slow exchange limit. The input parameters for the simulation of the benzylic methylene protons are listed in Table 4. The rate constant of complex **2** in acetone-d_6 was determined only at one temperature because the chemical shift difference was very small. The following input data were used for the analysis of the ethyl-methylene protons in the benzyl ethyl sulfide complexes: **4** $\Delta\nu_{AB}=0.112t+122.2$ Hz, $J_{AB}=-13.2$, $J_{AX}=J_{BX}=7.4$ Hz, $T_2=0.22$ s; **5** $\Delta\nu_{AB}=0.057t+18.3$ Hz, $J_{AB}=-12.6$, $J_{AX}=J_{BX}=7.3$ Hz, $T_2=0.23$ s. The rate constants obtained from the analysis are listed in Table 5.

MO Calculations. Ab initio calculations for gold complexes of dimethyl sulfide were carried out by the Gaussian 92 program[21)] on a convex computer. Total energies were calculated with the use of the LANL1DZ[22—24)] basis set without modification, which accommodated parameters for heavy atoms. The initial structures were made with reference to the X-ray structures of dibenzyl sulfide complexes.[25,26)] In calculation for the transition state, the sulfur atom was fixed at a planar geometry. The frequency analysis for the transition state structures gave one imaginary value for frequency number.

This work was partly supported by a Grant-in-Aid for Scientific Research on Priority Area of Reactive Organometallics No. 06227267 from the Ministry of Education, Science and Culture. The measurement of the 400 MHz NMR was performed at the Instruments Center, Okayama University of Science.

References

1) E. W. Abel, S. K. Bhargava, and K. G. Orrell, *Prog. Inorg. Chem.*, **32**, 1 (1984).

2) K. G. Orrell, *Coord. Chem. Rev.*, **96**, 1 (1989).

3) M. Ōki, *Pure Appl. Chem.*, **61**, 699 (1989).

4) M. Ōki, "Structure and Dynamics of Solution," ed by H. Ohtaki and H. Yamatera, Elsevier Science Publishers, Amsterdam (1992), Chap. 6.5.

5) M. Ōki and Y. Yamada, *Bull. Chem. Soc. Jpn.*, **61**, 1181 (1988).

6) M. Ōki and Y. Yamada, *Bull. Chem. Soc. Jpn.*, **61**, 1191 (1988).

7) S. Toyota, Y. Yamada, M. Kaneyoshi, and M. Ōki, *Bull. Chem. Soc. Jpn.*, **62**, 1509 (1989).

8) S. Toyota and M. Ōki, *Bull. Chem. Soc. Jpn.*, **64**, 1563 (1991).

9) F. Coletta, R. Ettorre, and A. Gambaro, *Inorg. Nucl. Chem. Lett.*, **8**, 667 (1972).

10) M. Nakamura, H. Kihara, N. Nakamura, and M. Ōki, *Org. Magn. Reson.*, **12**, 702 (1979).

11) M. Ōki, "Applications of Dynamic NMR Spectroscopy to Organic Chemistry," VCH Publishers, Deerfield Beach (1985).

12) T. Morita and M. Ōki, *Bull. Chem. Soc. Jpn.*, **61**, 1185 (1988).

13) P. C. Ray and D. C. Sen, *J. Indian Chem. Soc.*, **7**, 67

(1930).

14) F. Herrmann, *Ber.*, **38**, 2813 (1905).

15) A modified version of DNMR3 program[16)]for NEC-PC98 series computers by Dr. Kihara of Hyogo University of Teacher Education.

16) G. Binsch, *Top. Stereochem.*, **3**, 97 (1968).

17) D. J. Gulliver, W. Levason, K. G. Smith, M. J. Selwood, and S. G. Murray, *J. Chem. Soc.*, *Dalton Trans.*, **1980**, 1872.

18) K. Takahashi and H. Tanino, *Chem. Lett.*, **1988**, 641.

19) F. H. Brain, C. S. Gibson, J. A. J. Jarvis, R. F. Phillips, H. M. Powell, and A. Tyabji, *J. Chem. Soc.*, **1952**, 3686.

20) C. Janiak and R. Hoffmann, *Inorg. Chem.*, **28**, 2743 (1989).

21) "Gaussian 92, Revision C," M. J. Frisch, G. W. Trucks, M. Head-Gordon, P. M. W. Gill, M. W. Wong, J. B. Foresman, B. G. Johnson, H. B. Schlegel, M. A. Robb, E. S. Replogle, R. Gomperts, J. L. Andres, K. Raghavachari, J. S. Binkley, C. Gonzalez, R. L. Martin, D. J. Fox, D. J. Defrees, J. Baker, J. J. P. Stewart, and J. A. Pople, Gaussian, Inc., Pittsburgh (1992).

22) P. J. Hay and W. R. Wadt, *J. Chem. Phys.*, **82**, 270 (1985).

23) W. R. Wadt and P. J. Hay, *J. Chem. Phys.*, **82**, 284 (1985).

24) P. J. Hay and W. R. Wadt, *J. Chem. Phys.*, **82**, 299 (1985).

25) K. Takahashi, *Bull. Chem. Soc. Jpn.*, **64**, 2572 (1991).

26) J. Strähle, W. Hiller, and W. Conzelmann, *Z. Natureforsch.*, *B*, **39**, 538 (1984).

27) W. J. Hehre, L. Radom, P. v. R. Schleyer, and J. A. Pople, "Ab Initio Molecular Orbital Theory," John Wiley & Sons, Inc., New York (1986).